# Combined Radiofrequency Ablation and Acetic Acid-Hypertonic Saline Solution Instillation: An *In Vivo* Study of Rabbit Liver

Jeong Min Lee, MD[1, 2]
Young Kon Kim, MD[3]
Sang Won Kim, MD[3]
Joon Koo Han, MD[1, 2]
Se Hyung Kim, MD[1, 2]
Byung Ihn Choi, MD[1, 2]

**Objective:** We wanted to determine whether combined radiofrequency ablation (RFA) and acetic acid-hypertonic saline solution (AHS) instillation can increase the extent of thermally mediated coagulation in *in vivo* rabbit liver tissue. We also wished to determine the optimal concentration of the solution in order to maximize its effect on extent of the RFA-induced coagulation.

**Materials and Methods:** Forty thermal ablation zones were produced in 40 rabbits by using a 17-gauge internally cooled electrode with a 1-cm active tip under ultrasound guidance. The rabbits were assigned to one of four groups: group A: RFA alone (n=10); group B: RFA with 50% AHS instillation (n=10); group C: RFA with 25% AHS instillation (n=10); group D: RFA with 15% AHS instillation (n=10). A range of acetic acid concentrations diluted in 36% NaCl to a total volume of 1 mL were instilled into the liver before RFA. The RF energy (30 W) was applied for three minutes. After RFA, in each group, the maximum diameters of the thermal ablation zones in the gross specimens were compared. Technical success and the complications that arose were evaluated by CT and on the basis of autopsy findings.

**Results:** All procedures are technically successful. There were six procedure-related complications (6/40; 15%): two localized perihepatic hematomas and four chemical peritonitis. The incidence of chemical peritonitis was highest for group B with the 50% AHS solution instillation (30%). With instillation of 15% AHS solution, a marked decrease of tissue impedance (24.5 ±15.6 Ω) and an increase of current (250 mA) occurred as compared to RFA alone. With instillation of the solutions before RFA (group B, C and D), this produced a greater mean diameter of coagulation necrosis than the diameters for rabbits not instilled with the solution (group A) ($p < 0.05$). However, there was no significant difference between group B, C, and D.

**Conclusion:** Combined AHS instillation and RFA can increase the dimension of coagulation necrosis in the liver with a single application. A low concentration of AHS (15%) showed similar effects in increasing the extent of RF-induced coagulation, but there were less side effects as compared to the high concentration of AHS.

**Index terms:**
Liver interventional procedures
Experimental study
Radiofrequency (RF) ablation

***Korean J Radiol 2004;5:31-38***
Received October 19, 2003; accepted after revision February 9, 2004.

[1]Department of Radiology and [2]Institute of Radiation Medicine, Seoul National University College of Medicine, Seoul, Korea; [3]Department of Radiology, Chonbuk National University Medical School, Chonju, Korea

**Address reprint requests to:**
Jeong-Min Lee, MD, Department of Radiology, Seoul National University Hospital, 28, Yongon-dong, Chongno-gu, Seoul 110-744, Korea.
Tel. (822) 760-3154
Fax. (822) 743-6385
e-mail: leejm@radcom.snu.ac.kr

Radiofrequency ablation (RFA) is a localized treatment designed to destroy tumors by heating tissue to temperatures that exceed 60℃, and several studies have demonstrated that RFA provides a high rate of local tumor control (1–5). However, despite the technological advances and electrode modifications that have effectively increased radiofrequency (RF) energy deposition and tissue heating, several recent studies have reported inadequate treatment as a clinical problem for malignant liver tumors greater than 3 cm in

diameter (6−8). The cause of this has been suggested to be due to gross underablation of the tumors and the failure to create an adequate tumor free-margin (9).

Given the high likelihood of incomplete treatment with heat-based therapy alone, several adjuvant therapies have attempted to improve the efficacy of RFA by modifing the tumor's underlying physiologic characteristics. These therapies include the use of saline-enhanced RFA (10−13), combined with chemotherapy (14), chemoablation using ethanol or acetic acid (15, 16), and embolization (17). Among various possible adjunctive treatment strategies, combining RFA with chemoablation using ethanol or acetic acid seems to be attractive because given the minimally invasive characteristics of each procedure, both procedures could be performed at the same time and same place. Although a combined therapy of RFA and percutaneous injection of ethanol or acetic acid could increase the extent of induced coagulation necrosis, as compared with either therapy alone, instillation of ethanol or acetic acid into the target tissue before RFA could increase the tissue resistance to electrical flow. This can result in a decrease of current deposit and less heat production (15, 16). Lee et al (13) reported that hypertonic saline instillation before RFA more effectively achieved coagulation necrosis than RFA only by increasing the electrical tissue conductance. Given that acetic acid has similar cytotoxic effects on tumor cells as ethanol at a lower concentration (15%), and acetic acid is ionic and water soluble, the acetic acid-hypertonic saline (AHS) solution would be optimal for combining with RF ablation to induce synergistic effects for inducing coagulation necrosis (18−20).

The purpose of this investigation is to determine whether a combination of AHS solution and RFA can increase the extent of thermally mediated coagulation in *in vivo* rabbit liver tissue. We also wish to determine the optimal concentration of the AHS solution in order to maximize its effect on the dimension of the RFA-induced coagulation.

## MATERIALS AND METHODS

### Animal Preparation

The study was approved by the animal care committee of our institute. Forty New Zealand white rabbits weighing 3− 3.5 kg each were anesthetized using an intramuscular instillation of 50 mg/kg ketamine hydrochloride (Ketamine ®, Yuhan, Seoul, Korea) and 5 mg/kg xylazine (Rumpun®, Bayer Korea, Ansan, Korea) prior to the RFA and other procedures. Booster injections of up to one-half of the initial dose were administered as needed. After an adequate anesthesia was achieved, the epigastrium and back were shaved, sterilized and a wire mesh ground pad (10 cm ×15 cm) and conductive gel were placed on the animal's back.

Ten rabbits each were allocated into one of four groups: group A: standard RFA alone; group B: RFA with 1 mL of 50% AHS instillation; group C: RFA with 1mL of 25% AHS instillation; and group D: RFA with 1mL of 15% AHS instillation. Eight rabbits from each group were sacrificed on the day of the procedure. The remaining two rabbits of each group were sacrificed after undergoing a contrast-enhanced CT scan at 3 days after the procedure, in order to evaluate the histopathologic changes of the RF-induced ablation zones over time.

### RFA Setting and Ablation Protocol

One RFA-induced coagulation zone was created in the liver of each rabbit using a 500-kHz RF generator (series CC-3, Radionics, Burlington, Mass., U.S.A.) capable of delivering 200 W of power, and an internally cooled, 17-gauge electrode (Radionics, Burlington, Mass., U.S.A.) with a 1-cm active tip. A total of 40 ablation zones were produced with or without the AHS instillation. The electrode was placed in the central portion of the left lobe of the liver under ultrasound guidance, and a polyteflon-coated, 21-gauge Chiba needle (M.I.Tech, Seoul, South Korea) was then inserted using the tandem technique (21).

In group B, C, and D rabbits, 1 mL of different concentration of AHS was instilled slowly (over a period of 30 seconds) into the liver tissue before the RFA: 50% AHS in group B rabbits; 25% AHS in group C rabbits; and 15% AHS in group D rabbits. The timing of AHS instillation with the RFA was selected based on the results of previous experimental study regarding the combined therapy of RFA and percutaneous ethanol injection of (PEI) in rabbits, in which PEI followed by RFA created a greater extent of induced coagulation necrosis than RFA followed by PEI (15). To maximize the effects of the AHS instillation, the needle tip was placed 3 mm posterior to the tip of the RF electrode. The dose of AHS was selected based on a previous experimental study of combined RFA with acetic acid injection (16). The concentrations of AHS were chosen based on a clinical study of acetic acid instillation for treatment of hepatocellular carcinoma (18).

During the procedure, a thermocouple embedded within the electrode tip continuously measured the local tissue temperature. Tissue impedance was monitored by circuitry incorporated into the generator. A peristaltic pump (Watson-Marlow, Medford, Mass., U.S.A.) was used for infusing normal saline solution at 0℃ into the lumen of the electrodes at a rate sufficient to maintain a tip temperature of 20−25℃. The power output was set at 30 W, and the RF energy was applied for three minutes; these treatment

parameters were based on the results of a previous study (13, 16, 22). The applied current, power output, and impedance during RFA were continuously monitored by the by the instruments incorporated on the generator. The technical parameters of RFA (namely, impedance and current changes), the dimensions of the RFA coagulated area, and ensuing complications were compared for each group.

### Imaging Examination

A Spiral CT (Somatom Plus 4; Siemens, Erlangen, Germany) was performed with a 3-mm slice thickness and a 1.0 pitch. The CT scan included the entire liver field, before and after the contrast injection of 6–9 cc Ultravist 370®(Schering, Berlin, Germany) at a rate of 1 ml/sec through the ear vein in order to monitor the ablation effects immediately after RFA. Post-contrast CT scans were obtained 10, 30, and 60 seconds following the contrast administration. Two radiologists reviewed both the pre- and post-ablation CT images of all animals, and the radiologists had to reach a consensus in each case. Each RFA ablation zone was evaluated for its location, size, shape (round, oval or irregular), attenuation changes and the presence of hemorrhage in the peritoneal cavity. The findings on post-procedure CT images were compared with those on the pre-procedure CT images to ensure that the changes seen were not present before RFA.

### Histopathologic Studies and Measurements of Ablation Zones

The rabbits were sacrificed with an overdose injection of ketamine and xylazine after obtaining the post-procedure CT images and follow-up CT images. The specimens were dissected in planes similar to those of the spiral CT scans: a central cross-sectional incision was made through the affected area and a 3−6 mm parallel section was obtained from the ablation zone. Based on a previous study (22), for macroscopic examination, two observers measured the short-axis and long-axis diameters of the ablation zones, i.e, the central discolored region of coagulation necrosis, in each pathologic specimen with the use of calipers, and the two observers had to reach a consensus. Representative lesions were then fixed in 10% formalin for routine histologic processing, and the samples were finally processed with paraffin sectioning and hematoxylin-eosin (HE) staining for light microscopic study. Tissues from all treatment areas were analyzed for their histologic appearance and their clear demarcation from surrounding viable tissue. A surgical pathologist and a radiologist evaluated the gross and microscopic findings at each RFA site and a required consensus was reached.

### Statistical Analysis

For all the statistical analysis, SPSS 9.0 computer software (SPSS Inc., Chicago, Ill., U.S.A.) was used. A one-way analysis of variance with the Scheffe test was performed to compare the findings obtained with various concentrations of AHS instillation with those obtained without AHS instillation (23). For all the statistical analysis, a $p$ value of less than 0.05 was considered as statistically significant.

## RESULTS

### *Technical Parameters*

The mean initial tissue impedances were 117.1±18.6 Ω in group A and 117 ±20.3 Ω, 98.2 ±13.1 Ω and 93.5 ± 7.8 Ω, in group B, C, and D, respectively (Table 1). The difference in impedance value among groups A and C or groups A and D were statistically significant ($p < 0.05$). For groups A and B rabbits, the impedance rose gradually during application of RF energy, up to 200−450 Ω, and it induced a significant decrease of current flow below 200 mA during the procedure. However, for groups C and D, the impedance was decreased by instillation of 1 mL of the solution, and it was not markedly increased during RF energy application. Therefore, for groups C and D, the current flow of 400−700 mA was maintained during RF energy application.

### *Pathologic Findings*

#### Macroscopic findings

The RFA was technically successful in all test conditions. There were no deaths during RFA. After the RF treatment,

**Table 1. The Effect of Acetic Acid - Hypertonic Saline Injection on Tissue Impedance and Current in Normal Rabbit Liver**

| | Group A | Group B | Group C | Group D | $p$ Value |
|---|---|---|---|---|---|
| Initial tissue impedance | 117.1 ±19† | 113.6 ±15 | 110.6 ±12* | 112.4 ±20* | $p > 0.05$ |
| Impedance after infusion of AHS | N/A | 117 ±20† | 98.2 ±13*† | 93.5 ±8*† | $p < 0.05$*† |
| Mean current (mA) | 325.1 ±54‡ | 307.0 ±41.5 | 694.2 ±72‡ | 706.8 ±89‡ | $p < 0.05$ |

Note.—AHS: acetic acid-hypertonic saline solution. * the difference in tissue impedance before and after AHS infusion, †the differences in the tissue impedance in the three groups, ‡the differences in mean current in groups A and C and groups A and D.

a well-defined circular or oval ablation zone with white brown discoloration could be seen on the liver section of the ablation zone (Fig. 1). The mean long-axis diameters, as measured in the gross specimens of the four groups, were as follows: 12.3 ±1.2 mm in group A, 25.6 ±9.9 mm in group B, 25.4 ±9.5 mm in group C and 21.4 ±9.2 mm in group D (Table 2). The difference in long-axis diameters in group A and the other groups were statistically significant ($p < 0.05$). In addition, the mean short-axis diameters of the ablation zones in each group of rabbits are as

**Table 2. The Effect of Hypertonic Saline Injection on the Diameter of RF-Induced Coagulation Necrosis in Normal Rabbit Liver**

| Coagulation Necrosis | Group A | Group B | Group C | Group D | *p* Value |
|---|---|---|---|---|---|
| Long diameter (mm) | 12.3 ±1.2 | 25.6 ±9.9 | 25.4 ±9.5 | 21.4 ±9.2 | $p < 0.05$* |
| Short diameter (mm) | 11.1 ±0.9 | 20.7 ±6.4 | 17.4 ±3.4 | 16.5 ±6.7 | $p < 0.05$† |

Note.— *Differences in mean long-axis diameters between group A and other groups, †Differences in mean short-axis diameters between group A and other groups.

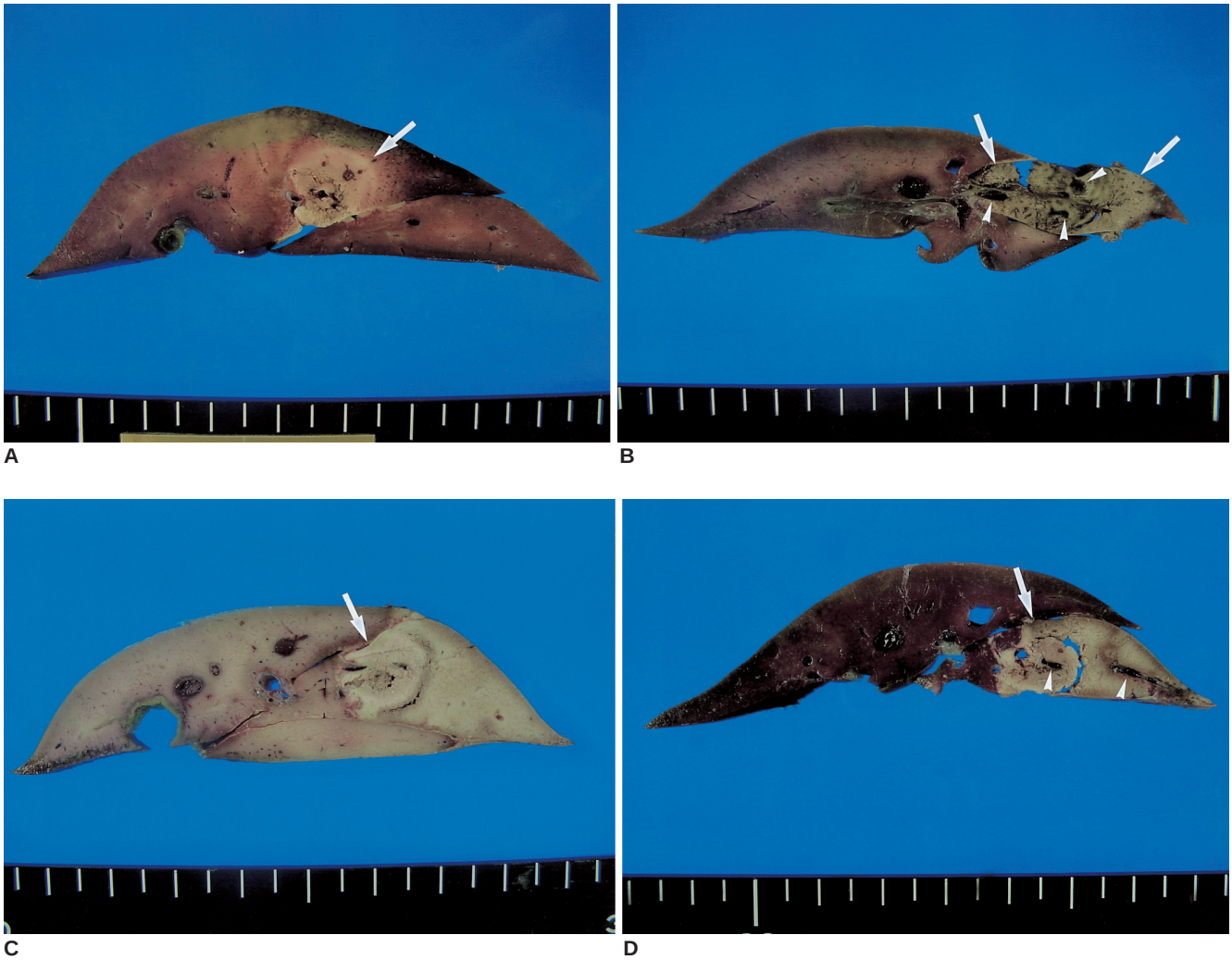


**Fig. 1.** Cut Sections of gross specimens in the four groups. In groups B, C, and D, the combined radiofrequency ablations with instillation of the acetic acid-hypertonic saline solutions produced greater ablation zones than that does radiofrequency alone (group A).
**A.** Gross specimen of a group A (radiofrequency ablation only) rabbit shows a round pale-discolored area (arrow) in the liver.
**B.** Gross specimen of a group B (radiofrequency ablation with 50% acetic acid instillation) rabbit shows an oval shaped discolored coagulation zone (arrows) and thrombosis (arrowheads) of small vessels within the zone.
**C.** Gross specimen of a group C (radiofrequency ablation with 25% acetic acid instillation) rabbit shows greater area of the ablation zone (arrow) than those of groups A (**A**) and B (**B**).
**D.** Gross specimen of a group D (radiofrequency ablation with 15% acetic acid instillation) rabbit shows a similar appearance with the ablation zone to group C. Note that the thrombosis of small vessels (arrowheads) are seen in the coagulation area (arrow).

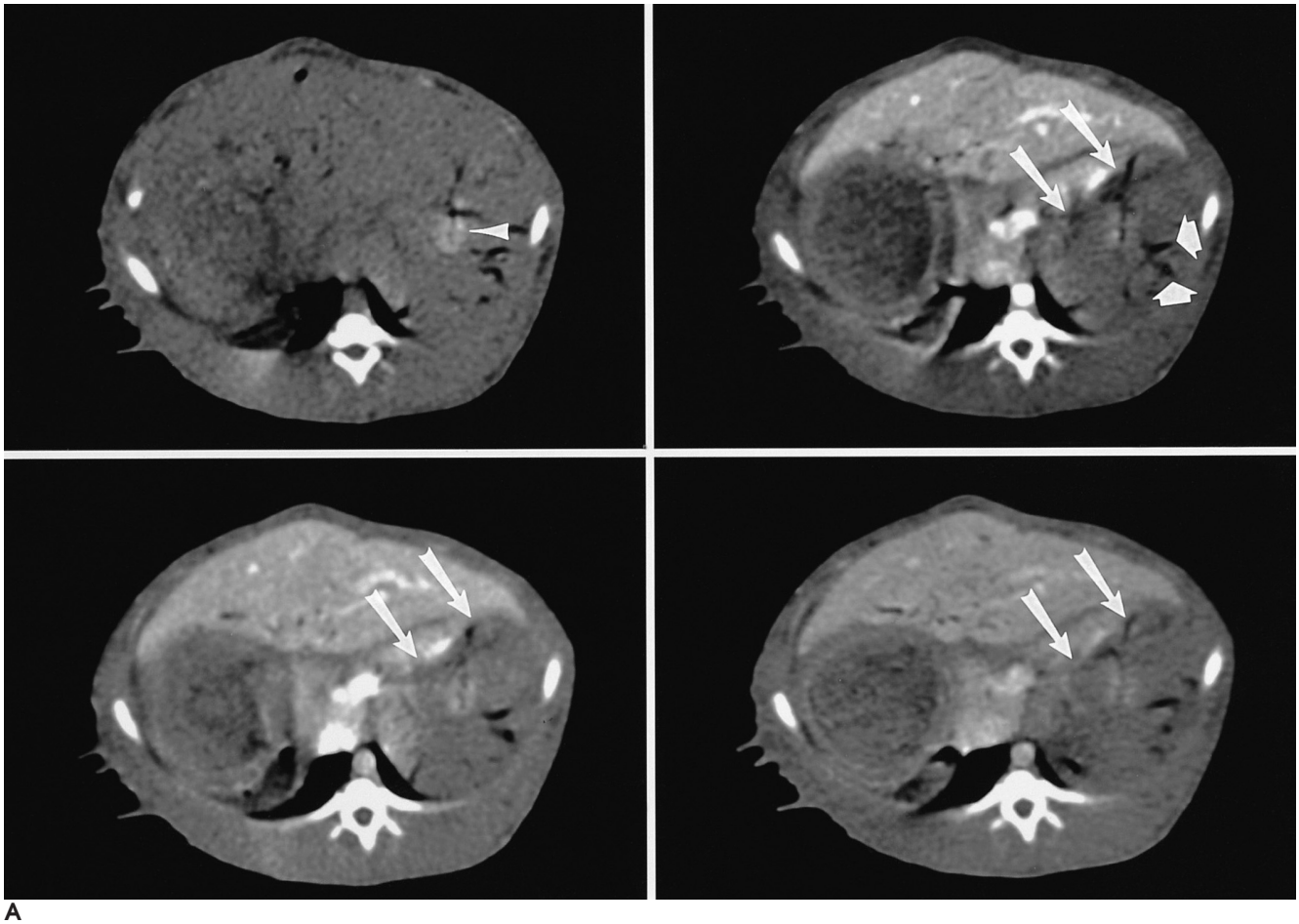

A

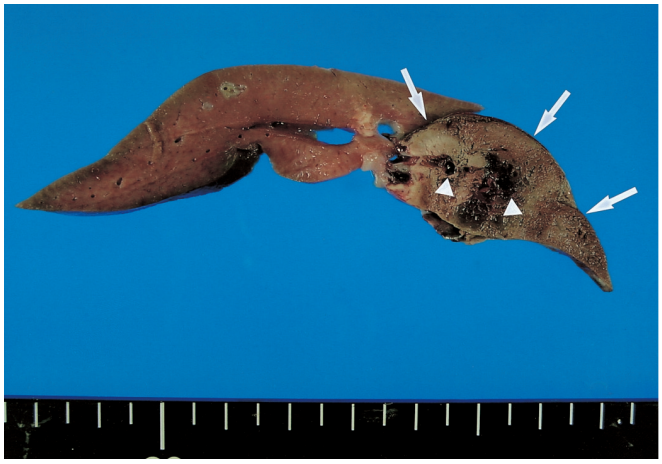

B

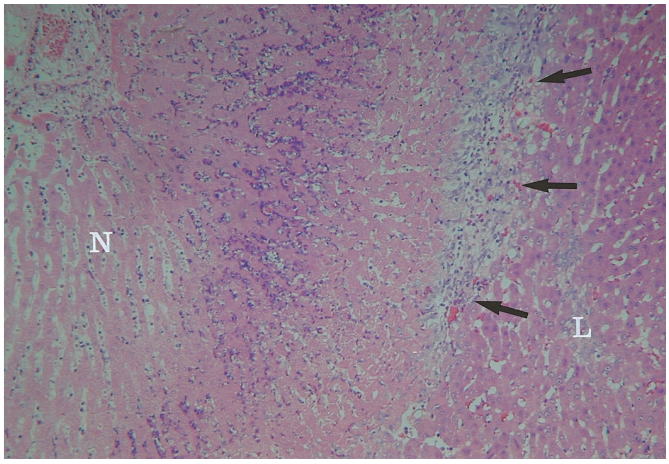


C

**Fig. 2.** Radiofrequency ablation with 25% acetic acid-hypertonic saline in a group C rabbit.
**A.** At post-procedural CT scanning, a 25-mm diameter, oval-shaped perfusion defect (arrow) is seen. Note the gas bubbles (arrowheads) in vessels within the ablation zone.
**B.** Gross specimen shows that the liver contains a white-brown colored coagulation zone (arrow) with an irregular margin. Note the thrombosis of hepatic vessels (arrowheads) within the coagulation area.
**C.** Microscopic image (original magnification, ×200; hematoxylin-eosin staining) shows a typical coagulation necrosis (N) of the ablated ablation zones, which is surrounded by fibroid tissue (arrows) and normal hepatocytes (L).

follows: 11.1 ±0.9 mm in group A; 20.7 ±6.4 mm in group B; 17.4 ±3.4 mm in group C; and 16.5 ±6.7mm in group D ($p < 0.05$). The difference in short-axis diameters for group A and other groups were statistically significant ($p < 0.05$). Therefore, AHS pretreatment with RFA in the groups B, C, and D produced larger dimensions of coagulation than those of the group A ($p < 0.05$). However, regardless of the concentration of acetic acid in solutions, there were no significant differences in long- axis diameter and short-axis diameters of the coagulation necrosis among groups B, C, and D ($p > 0.05$).

There were six procedure-related complications (15%) that were found on autopsy, i.e. two localized perihepatic hematomas and four chemical peritonitis inducing discolorization of liver capsule and a serosal surface of the stomach, and ascites. The localized perihepatic hematomas occurred in one of group C and D rabbits, respectively; the chemical peritonitis occurred in three of the group B rabbits and one of the group C rabbit; and there was no complication in groups A rabbits. Chemical peritonitis occurred more frequently for group B than for the other groups, although the difference was not statistically significant ($p > 0.05$).

**Microscopic Findings**

Histological examination of the RF-induced ablation zones showed a central charred zone with the complete destruction of the parenchyma, and this included a small central cavity where tissue had been lost (Fig.1). Surrounding this area were two zones of a white-yellow colored coagulation necrosis and a peripheral hemorrhagic rim. Microscopic examination of the ablation zones revealed a central zone of altered cellular morphology, which was best characterized as a heat effect (22); it consisted of degenerated, shrunken hepatocytes with pyknotic nuclei, and a peripheral zone of congestion and sinusoidal hemorrhage of the liver. In addition, the ablation zones of the rabbits that were sacrificed 3 days after RF ablation showed findings of typical coagulation necrosis upon histological examination (Fig. 2). The microscopic examination of the ablation zones of groups B, C and D with AHS instillation showed a thrombosis of the vessels within the ablated area (Figs. 1, 2).

***CT Findings***

After the procedure, the unenhanced CT scans revealed an indistinct zone of hyperattenuation extending from the site of the inserted electrode, and this hyperattenuated zone was surrounded by a slightly hypoattenuated zone. On contrast-enhanced CT scans, no contrast enhancement was seen in the region of the altered hepatic parenchymal attenuation (Fig. 2). The coagulated tissues were more conspicuous when observed after the contrast administration than was seen on the unenhanced CT scans. On the contrast-enhanced CT scans, gas bubbles were identified in the RF-induced nonenhanced areas of 24 rabbits (60%). On the contrast-enhanced CT scans, the ablation zones of groups B, C and D rabbits were more frequently irregular than those of group A rabbits; 30% (2/10) in group A vs. 63% (19/30) in groups B, C and D ($p < 0.05$) (Fig. 2).

## DISCUSSION

In this study, rabbits of groups B, C, and D (with the AHS instillation before RFA), showed larger dimensions of coagulation necrosis than the rabbits of group A (RFA alone) ($p < 0.05$). However, there was no difference among groups B, C, and D. This finding suggests that the increase of RF-induced coagulation necrosis might be related to both the cytotoxic effect of acetic acid (18, 19) and the improvement in electrical conductance by hypertonic saline (11, 12). Furthermore, the chemical peritonitis is related to leakage of acetic acid into peritoneal space (24). Therefore, the higher concentration of AHS used, the more complications could be occurred. Indeed, there was a tendency of high incidence rates (30%) of chemical peritonitis in rabbits with 50% AHS instillation than for rabbits of the other groups ($p > 0.05$). We believe that the use of a low concentration of AHS during RFA may have some potential merit for its clinical application in treating liver tumors, as compared to the use of a higher concentration of acetic acid.

Lee et al. (16) also described that the combined therapy of RFA and 50% acetic acid injection could induce larger area of coagulation necrosis than either therapy alone. Compared to the results of their study (16), the dimensions (> 20 mm) of coagulation necrosis achieved with combining RFA and AHS injection in groups B, C, and D were larger than those with 50% acetic acid (mean, 14.3 mm). Therefore, we believe that the effect of AHS injection before RFA to increase coagulation necrosis could be attributed to a synergistic effect of both therapies. The mechanisms of the synergistic effect of the two ablative therapies are most likely due to an improvement of electrical conductance and the elimination of the perfusion-mediated tissue cooling by inducing a thrombosis of small vessels of the treated tissue prior to RF heating (Fig. 1). Furthermore, we believe that AHS could be more suitable for achieving a synergistic effect with RFA than is ethanol or 50% acetic acid, and this is because of the low electrical conductance of those chemicals. Fifteen percent acetic acid has been reported to have the hepatocyte necrosis capabil-

ity equal to absolute alcohol, and it can be mixed with hypertonic saline too (18, 19). When mixing acetic acid with hypertonic saline, the cytotoxic effect is still maintained and electrical conductance can be further increased. In this study, with the instillation of 15% or 25% AHS, the tissue impedance decreased by more than 20 Ω. We can speculate that the decrease of tissue impedance after instillation of the AHS (15% and 25%) was related to a high concentration of ions in the 36% NaCl solution (11, 13).

Lee et al. (13) reported that RFA using hypertonic saline instillation with a single application could increase the volume of RFA-induced necrosis of the liver in rabbits, and that the increase of the ablation zone was related to the effect of increasing electrical conduction of hypertonic saline. Their study used the same RF equipment and parameters as our present study, and the mean long-axis diameters of coagulation necrosis that was created by hypertonic saline-enhanced RFA were much smaller than those of combined RFA with AHS instillations of this study: 14.9 mm vs. 25.6–21.4 mm. We can speculate that this difference is because acetic acid can reduce tissue perfusion by inducing small vessel thrombosis (18–20). These results were different from those of a previous study reported by Goldberg et al. (25), in which the addition of acetic acid injection to RFA substantially increased tumor destruction as compared with either therapy alone, but combined RFA and acetic acid injection produced a similar tumor coagulation to that of hypertonic saline-enhanced RFA. This could be explained by the differences in the tested animal and the vascularity of the target tissue.

It is a well-known fact that perfusion-mediated tissue cooling reduces the extent of coagulation produced by thermal ablation, and this is one of the major factors that limit dimensions of the ablation zone that achieved by RFA. Various methods to decreased tissue perfusion have been used to increase thermal ablation and they include the Pringle maneuver, angiographic balloon occlusion and pharmacologic modulation (8, 16, 26–29). Compared to other methods that decrease tissue perfusion, AHS instillation could be readily performed at the time of RFA, and moreover, the technique is also minimally invasive. Therefore, a combination of RF ablation and AHS instillation appears to be practical, very simple and easy to perform.

However, combining RFA and AHS instillation is apparently having some drawbacks as compared to RFA alone or hypertonic saline-enhanced RFA. First, one major drawback of a combined therapy of RFA and AHS instillation is the irregular shape of the ablation zones. The irregular shaped coagulation necrosis may be a result of uneven distribution of instilled AHS through the lower resistance tissue. This result is similar to the result of previous study of saline-enhanced RFA (10). PEI had achieved successful coagulation necrosis in cases of encapsulated hepatocellular carcinoma, but less desirable results have been obtained in cases of metastases (30, 31). This problem may not be a serious problem in cases of encapsulated hepatocellular carcinoma, yet it is serious drawback in cases of metastasis or infiltrative type hepatocellular carcinoma. Second, although no unwanted thermal injury occurred to other organs adjacent to the liverr such as stomach, colon or pancreas in our present study, there is the possibility of thermal injury to those organs if larger volumes of AHS instillation were used for the treatment of large size tumors.

There were some limitations to our study. First, rabbit livers are small and we therefore restricted the power of the RF energy to a lower level and shortened the time of the RF instillation as compared to the true clinical parameters (1–3, 8, 29). Therefore, the effects of the AHS solution could be underestimated in the clinical situation, and also the incidence rates of complications could have been underestimated. Second, the results obtained in normal liver tissue may differ from those obtained with malignant tumors in the human liver. However, according to previous studies regarding cell degeneration caused by the effect of heating on tissue (8, 32), we believe that the same results may have occurred with either normal liver tissue or human cancer cells. Third, at autopsy, we dissected the specimens along the planes similar to those of the spiral CT scans because it was very difficult to find a plane perpendicular to the axis of the electrode insertion. Therefore, the measured dimensions of the coagulation necrosis could be smaller than the real dimensions. Last, we tested only limited concentrations and amount of AHS, and we believe that further experimental study for the optimization of the concentration of AHS is warranted.

In conclusion, combined RFA with AHS instillation is more effective for achieving coagulation necrosis than RFA alone, and the lower concentration of AHS also shows a lower incidence of complications. Furthermore, since AHS instillation could be readily performed at the time of RFA, and since the technique is also minimally invasive, this combination therapy could be used for the management of large hepatic tumors.

*Acknowledgements*

The authors wish to thank Seon Ok Lee, R.T., for her assistance in animal observation, anesthesia and for her outstanding support in performing CT imaging.

## References


1. Gazelle GS, Goldberg SN, Solbiati L, Livraghi T. Tumor ablation with radio-frequency energy. *Radiology* 2000;217:633-646
2. Curley SA, Izzo F, Ellis LM, Vauthey JN, Vallone P. Radiofrequency ablation of hepatocellular cancer in 110 patients with cirrhosis. *Ann Surg* 2000;232:381-391
3. Curley SA, Izzo F, Delrio P, et al. Radiofrequency ablation of unresectable primary and metastatic hepatic malignancies: results in 123 patients. *Ann Surg* 1999;230:1-8
4. Dupuy DE, Goldberg SN. Image-guided radiofrequency tumor ablation: challenges and opportunities-part II. *J Vasc Interv Radiol* 2001;12:1135-1148
5. Lim HK. Radiofrequency thermal ablation of hepatocellular carcinomas. *Korean J Radiol* 2000;1:175-184
6. Livraghi T, Goldberg SN, Lazzaroni S, et al. Hepatocellular carcinoma: radiofrequency ablation of medium and large lesions. *Radiology* 2000;214:761-768
7. de Baere T, Elias D, Dromain C, et al. Radiofrequency ablation of 100 hepatic metastases with a mean follow-up of more than 1 year. *AJR Am J Roentgenol* 2000;175:1619-1625
8. Lim H, Goldberg SN, Dodd GD, et al. Essential techniques for successful radiofrequency thermal ablation of malignant hepatic tumors. *RadioGraphics* 2001;21:S17-S39
9. Dodd GD, Frank MS, Aribandi M, Chopra S. Chintapalli KN. Radiofrequency thermal ablation: computer analysis created by overlapping ablations. *AJR Am J Roentgenol* 2002;177:777-782
10. Livraghi T, Goldberg SN, Monti F, et al. Saline-enhanced radiofrequency tissue ablation in the treatment of liver metastases. *Radiology* 1997;202:205-210
11. Goldberg SN, Ahmed M, Gazelle GS, et al. Radio-frequency thermal ablation with NaCl solution injection: effect of electrical conductivity on tissue heating and coagulation-phantom and porcine liver study. *Radiology* 2001;219:157-165
12. Ahmed M, Lobo SM, Weinstein J, et al. Improved coagulation with saline solution pretreatment during radiofrequency tumor ablation in a canine model. *J Vasc Interv Radiol* 2002;13:717-724
13. Lee JM, Kim YK, Lee YH, Kim SW, Li CA, Kim CS. Percutaneous radiofrequency thermal ablation with hypertonic saline injection: *in vivo* study in a rabbit liver model. *Korean J Radiol* 2003;4:27-34
14. Kainumao O, Asano T, Aoyama H, et al. Combined therapy with radiofrequency thermal ablation and intra-arterial infusion chemotherapy for hepatic metastases from colorectal cancer. *Hepatogastroeneterology* 1999;46:1071-1077
15. Goldberg SN, Kruskal JB, Oliver BS, Clouse ME, Gazelle GS. Percutaneous tumor ablation: increased coagulation by combining radio-frequency ablation and ethanol instillation in a rat breast tumor modal. *Radiology* 2000;217:827-831
16. Lee JM, Lee YH, Kim YK, et al. Combined treatment of radiofrequency ablation and acetic acid injection: an *in vivo* feasibility study in rabbit liver. *Eur Radiol* 2004 (in press)
17. Rossi S, Garbagnati F, Lencioni R, et al. Percutaneous radiofrequency thermal ablation of nonresectable hepatocellular carcinoma after occlusion of tumor blood supply. *Radiology* 2000; 217:119-126
18. Ohnishi K, Ohyama N, Ito S, Fujiwara K. Small hepatocellular carcinoma: treatment with US-guided transtumoral injection of acetic acid. *Radiology* 1994;190:53-57
19. Liang HL, Yang CF, Pan HB, et al. Small hepatocellular carcinoma: safety and efficacy of single high-dose percutaneous acetic acid injection for treatment. *Radiology* 2000;214:769-774
20. Arrive L, Rosmorduc O, Dahan H, et al. Percutaneous acetic acid injection for small hepatocellular carcinoma: using CT fluoroscopy to evaluate distribution of acetic acid mixed with an iodinated contrast agent. *AJR Am J Roentgenol* 2003;180:159-162
21. Haaga JR. *Interventional CT-guided procedures.* In: Haaga JR, Lanzieri CF, eds. *Computed tomography and magnetic resonance imaging of the whole body*, 3rd ed. St.Louis: Mosby Yearbook, 1994:1572-1693
22. Lee JD, Lee JM, Kim SW, Kim CS, Mun WS. MR imaging-histopathologic correlation of radiofrequency thermal ablation lesion in a rabbit liver model: observation during acute and chronic stages. *Korean J Radiol* 2001;2:151-158
23. Lang TA, Secic M. *Analyzing multiple variables.* In: Lang TA, Secic M, eds. *How to report statistics in medicine*, 1st ed. Philadelphia: American College of Physicians, 1997:127-135
24. Koda M, Tanaka H, Murawaki Y, et al. Liver perforation: a serious complication of percutaneous acetic acid injection for hepatocellular carcinoma. *Hepatogastroenterology* 2000;47:1110-1112
25. Ahmed M, Weinstein J, Liu Z, et al. Image-guided percutaneous chemical and radiofrequency tumor ablation in an animal model. *J Vasc Interv Radiol* 2003;14:1045-1052
26. Goldberg SN, Gazelle GS, Mueller PR. Thermal ablation therapy for focal malignancy: a unified approach to underlying principles, techniques, and diagnostic imaging guidance. *AJR Am J Roentgenol* 2000;174:323-331
27. Patterson EJ, Scudamore CH, Owen DA, Nagy AG, Buczkowski AK. Radiofrequency ablation of porcine liver *in vivo*: effects of blood flow and treatment time on lesion size. *Ann Surg* 1998;227:559-566
28. Goldberg SN, Hahn PF, Halpern E, Fogle R, Gazelle GS. Radiofrequency thermal ablation: effect of pharmacologic modulation of blood flow on coagulation diameter. *Radiology* 1998; 209:761-769
29. McGahan JP, Dodd GD. Radiofrequency ablation of the liver: current status. *AJR Am J Roentgenol* 2001;176:3-16
30. Shiina S, Tagawa K, Niwa Y, et al. Percutaneous ethanol injection therapy for hepatocellular carcinoma: results in 146 patients. *AJR Am J Roentgenol* 1993;160:1023-1028
31. Livraghi T, Vettori C, Lazzaroni S. Liver metastases: results of percutaneous ethanol injection in 14 patients. *Radiology* 1991; 179:709-712
32. Nath S, Haines DE. Biophysics and pathology of catheter energy delivery systems. *Prog Cardiovasc Dis* 1995;37:185-204